ELSEVIER

Materials Science and Engineering A 394 (2005) 327–338

MATERIALS SCIENCE & ENGINEERING A

www.elsevier.com/locate/msea

Prediction of chemical stability in SiC_p/Al composites with alloying element addition using Wilson equation and an extended Miedema model

Tongxiang Fan*, Guang Yang, Di Zhang

State Key Lab of Metal Matrix Composites, Shanghai Jiaotong University, Shanghai 200030, PR China

Received 27 May 2004; accepted 18 November 2004

Abstract

Alloying additions have an important effect on the chemical stability of SiC_p/Al composites at high temperature. Using the Wilson equation and an extended Miedema model, the activity in a multiple-component system was calculated and then the influence of alloying element additions on the chemical reaction of SiC_p/Al composites at high temperature was investigated from a thermodynamic viewpoint. The calculation results showed that the addition of most alloying elements such as copper or silicon could reduce the interfacial chemical reaction but the addition of some alloying elements such as magnesium could promote the reaction. The experimental results were in agreement with the calculation results.

Keywords: Thermodynamics; Aluminum alloy; Analytical methods; Extended Miedema model

1. Introduction

Discontinuously reinforced metal matrix composites (DRMMCs) have been the subject of extensive research in the last two decades, particularly Al and Al alloy matrix composites reinforced with SiC particles (SiC_p/Al composites). Significant improvement in specific modulus and strength of SiC_p/Al composites is owed to load transfer from the matrix to the reinforcement through the interface. Thus, it is necessary to obtain a strong and chemistry-stable interface. However, when SiC_p/Al composites are fabricated by liquid processing [1–3], especially in remelt-recycling [4,5], the encountered chemical reaction usually is as follows:

$$[Al]_{liquid} + SiC \rightarrow Al_4C_3 + [Al–Si]_{liquid} \quad (1)$$

Water-soluble Al_4C_3 formed in the reaction can lead to the interfacial corrosion and dramatically decrease the mechanical properties of the resultant composites [6]. At the same time, the release of silicon results in undesirable physical and mechanical properties of the composite. Some investigations have shown that the extent of this interfacial reaction was dependent not only on the temperature and holding time but also on the use of adequate combinations of processing parameters. The amount of alloying elements can be an important factor influencing the stability of above chemical reaction [1,7,8].

Most research on the interfacial structure and thermodynamic equilibrium of the reaction above are for relatively pure metals and reinforcements. In practice, the metal is generally impure or alloyed, and the alloying additions can dramatically change the wetting angle or modify the characteristics of the oxide layer on the metal surface. For example, additions of Li into the Al matrix and the addition of Mg and Ti into Al–Sn alloys alter wetting of SiC [9,10]. Assuming a regular solution alloy and using statistical thermodynamic calculations, the influence of alloying addition on the wet ability of reinforcements to the matrix has been modeled by Li and coworkers [11,12]. The modeling could predict the influence of alloying addition on the wetting of the reinforcement particles at low dilution, and well agreed with experimental data.

When the aluminum alloy matrix is in a liquid state, most research has concentrated on experimentally carrying out measurements on the solid reaction products after the reac-

* Corresponding author. Tel.: +86 21 62933106; fax: +86 21 62822012.
E-mail address: txfan@mail.sjtu.edu.cn (T. Fan).

0921-5093/$ – see front matter © 2004 Elsevier B.V. All rights reserved.
doi:10.1016/j.msea.2004.11.040

tion. Few researchers have theoretically investigated how the interfacial reaction is influenced by alloying element additions in a liquid state and how to evaluate the silicon content formed in the reaction with different alloying contents, although Lee et al. has successfully predicted the silicon content required to prevent the formation of Al_4C_3, in some limited SiC_p/Al composites [13,14].

The component activity is an important factor in determining thermodynamic stability of the reaction between SiC reinforcement and Al matrix in liquid alloys. Thus, it is vital to understand this mechanism theoretically and thereby control it favorably, especially in a multiple-component system. Some theories based on the accumulated experimental data, mostly with the least-squares deviation method, have proved useful. With appropriate parameters, they can reproduce characteristic features of the activities of components and their variations with compositions and temperature. However, for ternary and n-component alloy systems for which $n > 3$, those data are very limited and it is expensive and time consuming to measure the component activities experimentally. As a result, the data for the ternary alloy systems are rather scarce and only a few quaternary and quinary alloy systems have been measured. For example, experimental data for the ternary Al–Si–X, where X represents some alloy component, is very limited [15]. Therefore, for the long term, there is a significant need for reliable theoretical calculation that can adequately represent expensive and lengthy experimental measurements.

Miedema's group has developed a widely used thermodynamic theory for calculating the formation energies of binary liquid alloys using physical parameters of the elements [16]. By combining an extended Miedema model with the Wilson equation [17], this paper presents an analytic expression for the thermodynamic activities in ternary alloy and predicts the chemical stability of the interfacial reaction between SiC reinforcement and Al matrix with alloying element additions above the liquidus.

2. Principle and experiment

2.1. Principle

For SiC_p/Al composites, kinetically, the interaction between Al and SiC includes the dissociation of SiC in molten aluminum, the diffusion of silicon and carbon ions away from the interface into the bulk liquid metal, and Al_4C_3 precipitation with increasing carbon activity in molten aluminum [8]. However, due to the low solubility of C into the pure Al even at high temperature (about 0.02–0.04 wt.% at 1300–1500 °C and essentially zero below 1100 °C [18,19]), the liquid melt model of the Al–Si–C ternary system and Al–Si–C–X quaternary system can be approximated by an Al–Si binary system and an Al–Si–X ternary system, respectively, where X represents alloying element.

In the reaction of Eq. (1), including liquid-state reactants and products, the Gibbs free energy ΔG is not only a function of temperature, but also dependent on the concentration of reactants and products. The activities of solid SiC and Al_4C_3 in molten Al can be considered as unity and ΔG can be expressed as follows:

$$\Delta G_1 = \Delta G^0_{T,P} + 3RT \ln a_{Si} - 4RT \ln a_{Al} \tag{2}$$

where $\Delta G^0_{T,P}$ is the standard Gibbs energy of formation and a is the activity of component in the composite melt. Here, $\Delta G^0_{T,P}$ can be written as follows [20]:

$$\Delta G^0_{T,P} = \Delta G^f_{Al_4C_3} - 3\Delta G^f_{SiC_\alpha} + 3\Delta G^{D->liquid}_{Si} \tag{3}$$

$\Delta G^f_{Al_4C_3}$ and $\Delta G^f_{SiC_\alpha}$ are the free energy change associated with the formation of α-SiC and Al_4C_3, and $\Delta G^{D->liquid}_{Si}$ is the free energy change associated with the phase transformation of solid Si having a diamond crystallographic structure into the liquid phase.

When alloying element X is added into an aluminum matrix, the composite melt model can be approximated by an Al–Si–X ternary system. The influence of alloying element on the reaction can be considered from two aspects: (i) most alloying additions can promote reaction between the reinforcement and the matrix because they improve wetting of the reinforcement; (ii) the activities of Al and Si can be changed with alloying element addition. Therefore, for the alloy matrix in liquid state, the second factor is the dominant influence on the extent of the reaction. Therefore, with alloying addition, Eq. (2) can be rearranged as follows:

$$\begin{aligned}\Delta G_2 &= \Delta G^0_{T,P} + 3RT \ln(a_{Si} + \Delta a_{Si}) - 4RT \ln(a_{Al} + \Delta a_{Al}) \\ &= \Delta G^0_{T,P} + 3RT \ln(x_{Si} + \Delta x_{Si})(\gamma_{Si} + \Delta\gamma_{Si}) - 4RT \ln(x_{Al} + \Delta x_{Al})(\gamma_{Al} + \Delta\gamma_{Al}) \\ &= \Delta G_1 + 3RT \ln(1 + P_{Si})(1 + Q_{Si}) - 4RT \ln(1 + P_{Al})(1 + Q_{Al})\end{aligned} \tag{4}$$

where $a_i = x_i\gamma_i$, x_i represents the atom fraction of component i in the melt, and γ_i is the activity coefficient. Δx_i and $\Delta\gamma_i$ represent the values of the changes of the component concentration and activity coefficient, respectively, after alloying element addition. P_i and Q_i are denoted as follows:

$$P_i = \frac{\Delta x_i}{x_i}, \quad Q_i = \frac{\Delta\gamma_i}{\gamma_i} \tag{5}$$

Therefore, the influence of alloying element addition on interfacial stability at high temperature is determined mainly by both P_i and Q_i. P_i is easy to obtain through the alloying addition content, and once Q_i is determined, ΔG_2 can be calculated. However, Q_i is difficult to calculate owing to the complex influence of alloying element additions on γ_i.

Wilson introduced one method to calculate γ_i in multiple components as follows:

$$\ln\gamma_i = -\ln\left(1-\sum_j x_j A_{j/i}\right) + 1 - \sum_j \left(\frac{x_j(1-A_{i/j})}{1-\sum_k x_k A_{k/j}}\right) \tag{6}$$

where x_i is the molar fraction of component i and $A_{i/j}$ and $A_{j/i}$ are adjustable parameters. From the Wilson equation, the activity of ternary or higher components can be investigated using only parameters obtained from binaries.

In binary system, Eq. (6) can be rearranged as:

$$\ln\gamma_i = 1 - \ln(1-x_j A_{j/l}) - \frac{x_i}{1-x_j A_{j/i}} - \frac{x_j(1-A_{i/j})}{1-x_i A} \tag{7}$$

Furthermore, in a ternary system

$$\ln\gamma_i = 1 - \ln(1-x_j A_{j/i} - x_k A_{k/i}) - \frac{x_i}{1-x_j A_{j/i} - x_k A_{k/i}} - \frac{x_j(1-A_{i/j})}{1-x_i A - x_k A_{k/j}} - \frac{x_k(1-A_{i/k})}{1-x_i A_{i/k} - x_j A_{j/k}} \tag{8}$$

The pair of parameters, $A_{i/j}$ and $A_{j/i}$, could be obtained through the values of $\ln\gamma_i^{x_i\to 0}$ and $\ln\gamma_j^{x_j\to 0}$ based on the binary infinitely dilute activity coefficients [21] as follows:

$$\ln\gamma_i^{x_i\to 0} = -\ln(1-A_{j/i}) + A_{i/j} \tag{9}$$

$$\ln\gamma_j^{x_j\to 0} = -\ln(1-A_{i/j}) + A_{j/i} \tag{10}$$

The values of $\ln\gamma_i^{x_i\to 0}$ and $\ln\gamma_j^{x_j\to 0}$ can be obtained from experimental data. However, considering the limited experimental data, theoretic calculation is proposed in the present work using an extended Miedema model as is explained hereafter.

In Miedema model, the heat of formation, ΔH_{ij}, in binary liquid i–j alloy system can be deducted as

$$\Delta H_{ij} = f_{ij}\frac{x_i[1+u_i x_j(\varphi_i-\varphi_j)]x_j[1+u_j x_i(\varphi_j-\varphi_i)]}{x_i[1+u_i x_j(\varphi_i-\varphi_j)]V_i^{2/3} + x_j[1+u_j x_i(\varphi_j-\varphi)_i]V_j^{2/3}} \tag{11}$$

where

$$f_{ij} = \frac{2pV_i^{2/3}V_j^{2/3}\{q/p[(n_{ws}^{1/3})_i - (n_{ws}^{1/3})_j]^2 - (\varphi_i-\varphi_j)^2 - b(r/p)\}}{(n_{ws}^{1/3})_i^{-1} + (n_{ws}^{1/3})_j^{-1}} \tag{12}$$

In Eqs. (11) and (12), φ is the electron density and V is the molar volume. For all alloys q/p equals $9.4V^2/(du)^{2/3}$. The values for p, used in calculating numerical of f_{ij} in the Miedema model are $P = 14.1$, 10.6 and 12.3 (φ is in volts, n_{ws} in density units, V in cm^3, enthalpies in kJ/mol) for alloys of two transition metals, two non-transition metals, and a transition metal with a non-transition metal, respectively. b equals 1.0 for solid alloys and 0.73 for liquid alloys of a transition metal with a non-transition metal, and b equals 0 for the others alloys.

In an i–j binary liquid alloy system, the excess molar Gibbs free energy of component i, ΔG_i^E, can be expressed as

$$\Delta G_i^E = RT\ln\gamma_i \tag{13}$$

and the relation between ΔG_i^E and the whole excess molar Gibbs free energy, G_{ij}^E, in a binary system is given by

$$\Delta G_i^E = G_{ij}^E + (1-x_i)\frac{\partial G_{ij}^E}{\partial x_i} \tag{14}$$

and

$$G_{ij}^E = \Delta H_{ij} - TS_{ij}^E \tag{15}$$

The excess entropy of mixing can be approximately expressed as [22]

$$S_{ij}^E = 0.1\times\Delta H_{ij}\left(\frac{1}{T_{m_i}} + \frac{1}{T_{m_j}}\right) \tag{16}$$

where T_{m_i} represents the melting point of component i and T is the temperature of the liquid melt. From Eqs. (11)–(16), the activity coefficient of component i can be calculated as

$$\ln\gamma_i = \frac{\alpha_{ij}\Delta H_{ij}}{RT}\left\{1+(1-x)\left[\frac{1}{x_i} - \frac{1}{1-x_i} - \frac{u_i(\varphi_i-\varphi_j)}{[1+u_i(1-x_i)(\varphi_i-\varphi_j)]} + \frac{u_j(\varphi_j-\varphi_i)}{[1+u_j x_i(\varphi_j-\varphi_i)]} - \frac{V_i^{2/3}[1+u_i(1-2x_i)(\varphi_i-\varphi_j)] + V_j^{2/3}[1+u_j(1-2x_i)(\varphi_j-\varphi_i)]}{x_i V_i^{2/3}[1+u_i(1-x_i)(\varphi_i-\varphi_j)] + (1-x_i)V_j^{2/3}[1+u_j x_i(\varphi_j-\varphi_i)]}\right]\right\} \tag{17}$$

Here α_{ij} is denoted as

$$\alpha_{ij} = 1 - 0.1T\left(\frac{1}{T_{m_i}} + \frac{1}{T_{m_j}}\right) \tag{18}$$

Therefore, from Eq. (17), the activity coefficient of component i in infinite solution j can be deduced as:

$$\ln\gamma_i^{x_i\to 0} = \frac{\alpha_{ij}f_{ij}[1+u_i(\varphi_i-\varphi_j)]}{RTV_j^{2/3}} \tag{19}$$

Then, connecting Eqs. (4), (6), (9), (10) and (19), the chemical stability of Eq. (1) can be theoretically calculated when $\Delta G_2 < 0$. The advantage of this method is that, independent of experimental data, it is applicable for multiple liquid alloys and can predict the thermodynamic data according to the physical parameters of these elements. The reliability of this method will be discussed in Appendix A.

2.2. Experimental procedure

The SiC_p/Al composites used in the verification experiment were fabricated by vacuum-high pressure infiltration processing. The matrixes are pure Al, Al–1 wt.%Mg, Al–4 wt.%Mg, Al–2 wt.%Cu and Al–4.5 wt.%Cu, respectively. The dominant phase of SiC reinforcement was α-phase and its average size was about 7 μm and the reinforcement volume fraction was 15%.

Experimental verification was carried out by monitoring the equilibrium silicon content in SiC_p/Al composites by means of the in situ remelting methods described in the previous works [4,8]. In these works, the equilibrium Si content was evaluated from the liquidus temperatures exactly. Differential scanning calorimetry (DSC) was used to survey the liquidus temperature of composite melts in the present work. The samples were cut into discs of ϕ4 mm × 4 mm and the composite samples were remelted in a high purity alumina pan in a Netsch DSC404 instrument. Multiple runs were carried out at a heating rate of 20 °C/min from ambient to 850 °C, then cooling to ambient temperature at 20 °C/min under dynamic high purity argon atmosphere (80 ml/min), and high purity corundum was used as a reference. In order to make the reaction reach equilibrium, multiple remelting runs were performed with the DSC.

3. Results and discussion

3.1. Calculation results

3.1.1. SiC_p/pure Al composites

The values of the parameters required are presented in Table 1, and Table 2 lists the values of $A_{Al/Si}$ and $A_{Si/Al}$ at different temperatures in the Al–Si binary alloy system. Hence, the activity coefficients of aluminum and silicon in the Al–Si liquid alloy can be described as a function of concentration of components from Eq. (7). Fig. 1 shows the calculated activities of Al and Si at 1427 °C. Compared with the experimental data [23], the calculated activities at 1427 °C in the Al–Si binary system agreed well with the experimental results using the Wilson equation and the extended Miedema model.

In SiC_p/Al composites, when the interfacial reaction between Al and SiC reaches equilibrium, the Si content in molten Al matrix remains constant. Based on the thermodynamic model of the melt in SiC/pure Al composites in Eq. (2), the equilibrium silicon content can be calculated as a function of temperature, as seen in Fig. 2. Compared with other research, the calculation is close to the experimental results of Ferro and coworkers [24,25] but lower than the calculation results of Lee [13] using Barin's data and of Naisco and coworkers [26,27]. In addition, it can be seen from Fig. 2 that the equilibrium silicon content calculated at 850 °C is about 8.83 wt.%, which suggests that the addition of 8.83 wt.% Si

Table 1
The values of some parameters used in the calculations [16]

	$n_{ws}^{1/3}$ ((du)$^{1/3}$)	φ (V)	$V^{2/3}$ (cm^2)	T_m (K)	μ	r/p
Al	1.39	4.2	4.6	933	0.07	1.9
Si	1.50	4.7	4.2	1685	0.04	2.1
Mg	1.17	3.45	5.8	922	0.10	0.4
Cu	1.47	4.55	3.7	1357	0.04	0.3
Zn	1.32	4.1	4.4	693	0.04	1.4
Ge	1.37	4.55	4.6	1211	0.04	2.1
Sn	1.24	4.15	6.4	505	0.04	2.1
Ca	0.91	2.55	8.8	1115	0.10	0.4
Sr	0.84	2.4	10.2	1042	0.04	0.4
La	1.09	3.05	8.0	1191	0.04	0.7
V	1.64	4.25	4.1	2183	0.04	1.0
Co	1.75	5.1	3.5	1768	0.04	1.0
Fe	1.77	4.93	3.7	1811	0.04	1.0
Mn	1.61	4.45	3.8	1519	0.04	1.0
Sc	1.27	3.25	6.1	1814	0.04	0.7
Cr	1.73	4.65	3.7	2136	0.04	1.0
Ni	1.75	5.2	3.5	1728	0.04	1.0

Table 2
The values of the parameters $A_{Al/Si}$ and $A_{Si/Al}$ calculated at different temperature

T (°C)					
650	750	850	950	1050	1427
$A_{Al/Si}$					
−6.2370	−5.4239	−4.8074	−4.3219	−3.9281	−2.9231
$A_{Si/Al}$					
0.9946	0.9891	0.9817	0.9726	0.9621	0.9140

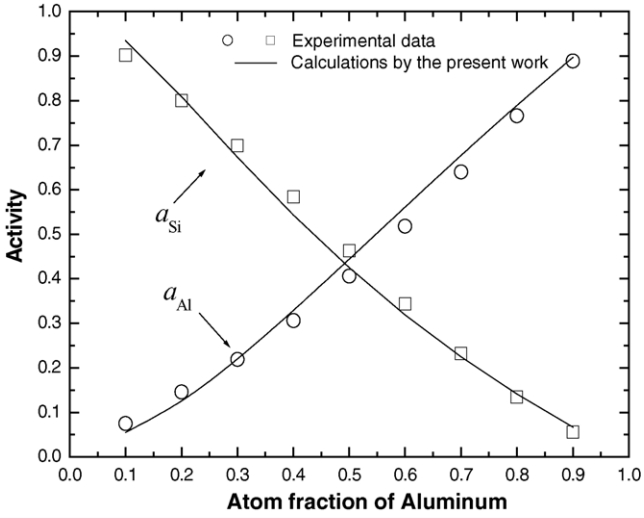

Fig. 1. Activities in liquid Al–Si alloys at 1427 °C.

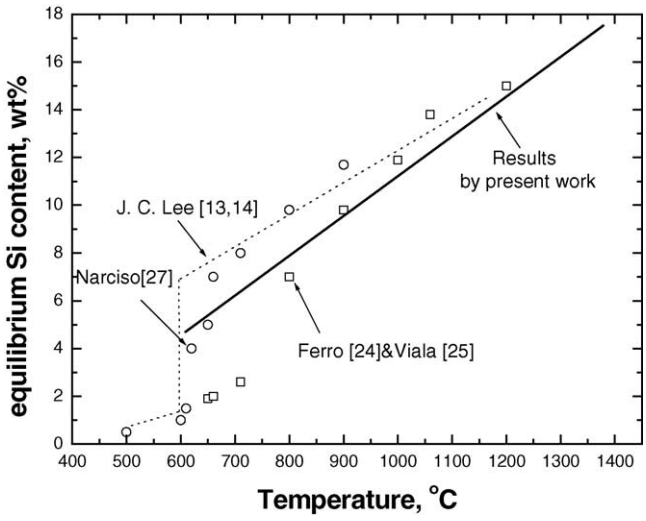

Fig. 2. Variation in the equilibrium Si content in SiC_p/Al composites plotted as a function of temperature.

into the Al-matrix can effectively suppress the reaction between Al and SiC reinforcement below 850 °C.

3.1.2. SiC_p/Al alloy composites

When the Al matrix includes alloying components, based on Eq. (8), the investigation on the influence of alloying element additions on the chemical stability of Eq. (1) can be divided into two aspects: (i) the variation P_i of component concentration in the composite melt, and (ii) the impact factor Q_i on activity coefficients of Al and Si. In SiC_p/Al–X alloy composites, such a composite melt at high temperature can be described as an Al–Si–X ternary liquid alloy system when the chemical reaction in Eq. (1) takes place. Thus, some parameters, i.e., $A_{Al/Si}$, $A_{Si/Al}$, $A_{Al/X}$, $A_{X/Al}$, $A_{X/Si}$, and $A_{Si/X}$, must be obtained using the Wilson equation from an interactive binary system. Following the calculation method of $A_{Al/Si}$ and $A_{Si/Al}$ and referring to the Table 1, the other four parameters can be solved from binary Al–X and Si–X alloys. The calculation results at 850 °C are shown in Table 3.

Fig. 3 shows the variation of activity coefficient of aluminum with the fraction of different alloying additions at the beginning stage of the interfacial reaction; silicon content tends to approach zero in the Al alloy solution. The results indicate that different alloying additions can result in different variations of $\gamma_{Al}^{x_{Si}\to 0}$ due to distinct physical characteristics of alloying elements. With the alloying content increasing, most of alloying addition such as Cu, Mn, Ti, La, etc., can decrease the activity coefficient of Al to different extents. On the contrary, although the effect is very small, the addition of Sn can increase $\gamma_{Al}^{x_{Si}\to 0}$. In addition, Mg and Zn additions have few effects on $\gamma_{Al}^{x_{Si}\to 0}$. When Al alloy is at solid state with the increasing alloying content at 850 °C, the results are plotted in the dotted curves, as seen in Fig. 3 and the following figures. The area of the dotted curves will decrease with the temperature increasing due to the melting point of

Table 3
The values of the parameters $A_{i/j}$ and $A_{j/i}$ calculated at 850 °C

X	$A_{Al/X}$	$A_{X/Al}$	$A_{Si/X}$	$A_{X/Si}$
Cu	−2.6392	−1.7642	−2.3421	−1.6943
Mg	0.9461	−3.5546	−1.6772	−2.3293
Ni	−6.5136	−5.0579	−9.2001	−7.5151
Nb	−5.6748	−6.0508	−12.1081	−13.8903
Cr	−2.5992	−2.2009	−6.3289	−5.1560
Sc	−12.3081	−15.4863	−18.7434	−25.4924
Ca	−1.3631	−3.1192	−4.3645	−8.3091
Sr	−0.6135	−2.5648	−3.3356	−8.0097
V	−4.4863	−3.7068	−9.7723	−8.9929
Fe	−2.9492	−2.2195	−5.2944	−4.2910
Ge	0.6135	−1.0563	0.4199	0.3075
Zn	0.0379	0.1356	−2.0821	−0.8329
Co	−4.5801	−3.3756	−5.6051	−4.3833
Mn	−5.5432	−4.1223	−8.9130	−7.5124
Ti	−9.4635	−9.6927	−16.7538	−17.8109
La	−14.0706	−24.7587	−10.7685	−20.6370
Sn	0.6512	0.2543	0.8282	0.5214

the alloys rising. Fig. 4 shows the corresponding values of Q_{Al} varying with the alloy content. When the value of Q_{Al}^{X} is higher, it means that the effect of the alloying element X on γ_{AL} is greater. It can be indicated from Fig. 4 that among those alloying elements that can reduce activity coefficient of aluminum, La has the greatest effect on $\gamma_{Al}^{x_{Si}\to 0}$, followed by Sc, Ti, Nb, Ni, Mn, and so on. For example, when 4 at.% La is added into molten Al at 850 °C, Q_{Al}^{La} equals about −0.175 and $Q_{Al}^{La} > Q_{Al}^{Sc} > Q_{Al}^{Ti} > Q_{Al}^{Nb}$, which means that the order influencing $\gamma_{Al}^{x_{Si}\to 0}$ is La, Sc, Ti, Nb, and Ni.

The influence of alloying additions on $\gamma_{Si}^{x_{Si}\to 0}$ in liquid Al alloys is shown in Fig. 5 and the corresponding values of Q_{Si} are shown in Fig. 6. As was the case with Q_{Al}^{X}, when the value of Q_{Si}^{X} is higher, the effect of the alloying element X on γ_{Si} is greater. It can be seen that most of alloying additions can decrease $\gamma_{Si}^{x_{Si}\to 0}$, which means that $Q_{Si} < 0$. Among such elements, Mg has the greatest effect on $\gamma_{Si}^{x_{Si}\to 0}$ and Q_{Si}^{Mg} is close to −0.825 with 10 at.% Mg addition in molten Al at

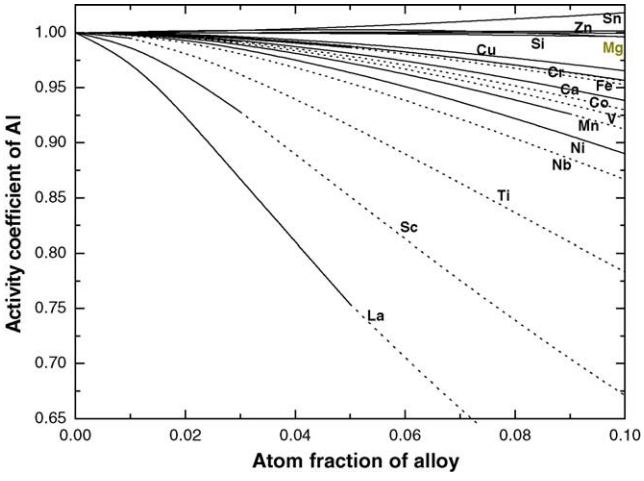

Fig. 3. Variation of activity coefficient of Al (Si% = 0) at 850 °C.

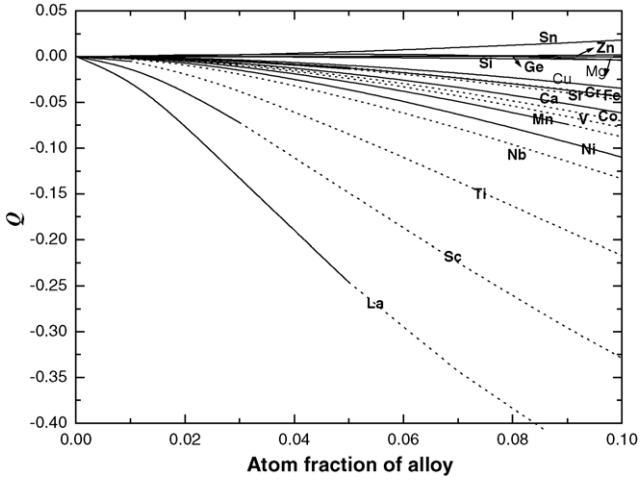

Fig. 4. Variation of Q_{Al} with adding alloy content at 850 °C (Si% = 0).

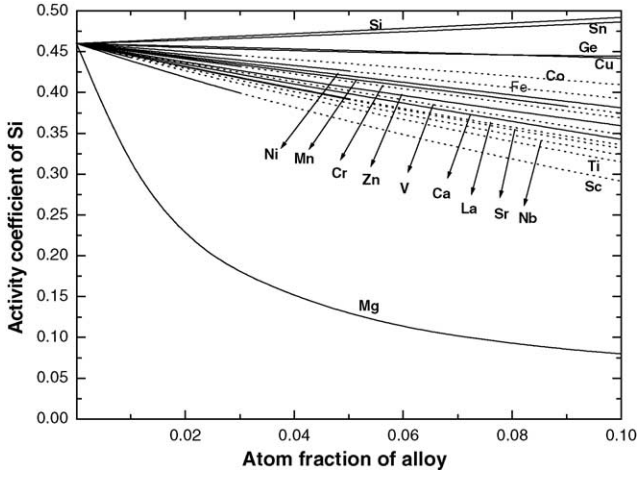

Fig. 5. Variation of activity coefficient of Si at 850 °C (Si% = 0).

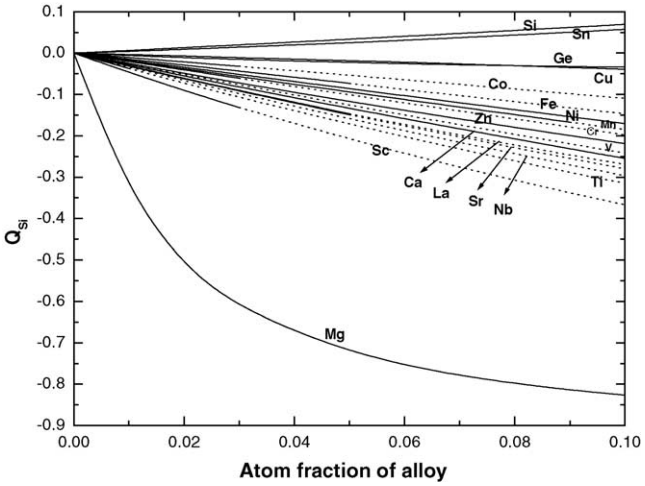

Fig. 6. Variation of Q_{Si} with adding alloy content at 850 °C (Si% = 0).

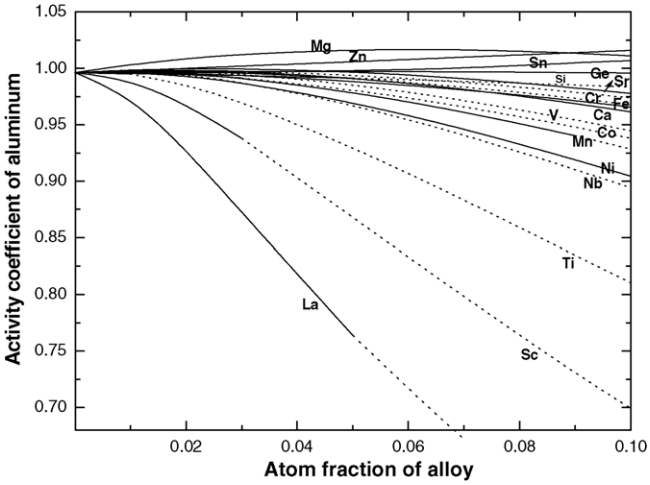

Fig. 7. Variation of activity coefficient of Al at 850 °C (assuming Si released from the reaction is about 10 at.%).

850 °C, and the next is Sc, Ti, Ni, La, etc. In addition, only a few alloying elements, including Sn and Si, can increase $\gamma_{Si}^{x_{Si}\to 0}$ and the effect is very small. For example, both Q_{Si}^{Sn} and Q_{Si}^{Si} are less than 0.1 with 10 at.% Sn and Si, respectively, added to molten Al at 850 °C.

When the rate of silicon release from the reaction increases, compared with the beginning stage, there may be some difference in the influence of alloying addition on γ_{Al} and γ_{Si}. Assuming that silicon content formed from the chemical reaction in the composites melt reaches 10 at.%, which is close to the content of the equilibrium silicon, Figs. 7–10 show the influence of alloying element additions on γ_{Al} and γ_{Si} and corresponding values of Q_{Al} and Q_{Si}. In contrast to the beginning stage (Si content is approximately 0), most absolute values of Q_{Al} and Q_{Si} decrease with increasing silicon content. For example, when alloying element content is at 10 at.%, Q_{Al}^{Ni} decreases from −0.110 to −0.090 and Q_{Si}^{Mg} de-

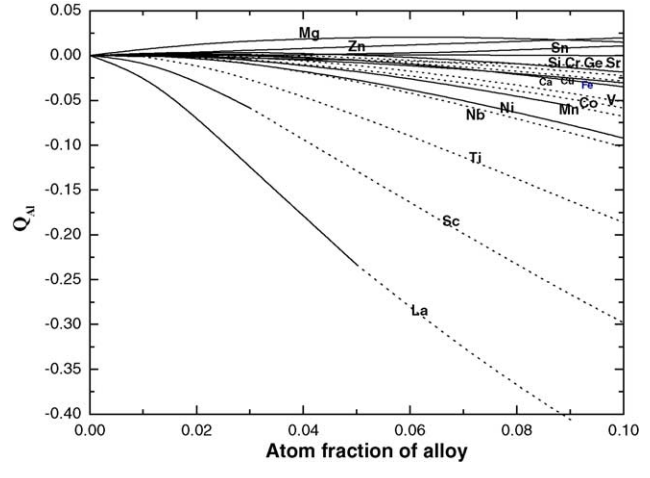

Fig. 8. Variation of Q_{Al} with adding alloy content at 850 °C (assuming Si released from the reaction is about 10 at.%).

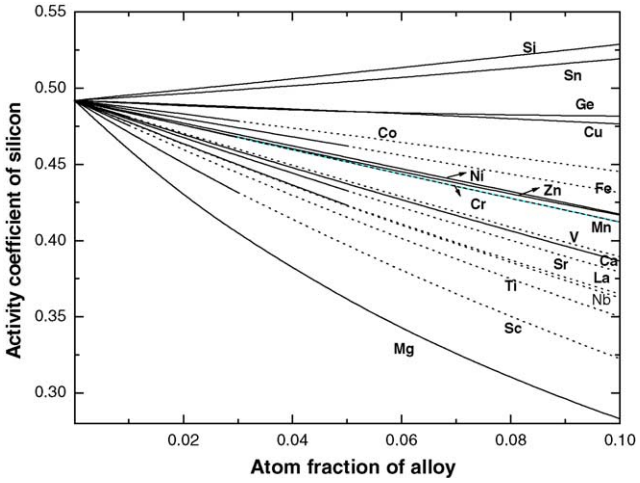

Fig. 9. The variation of activity coefficient of Si at 850 °C (assuming Si released from the reaction is about 10 at.%).

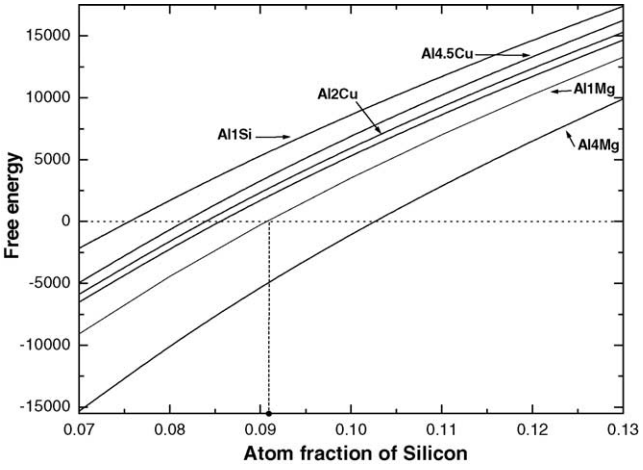

Fig. 11. Relationship between free energy and Si content formed in the chemical reaction at 850 °C.

creases from −0.825 to −0.425. In addition, in general, the order of influence of different alloying element additions is similar to that at the beginning stage and the negativity or positivity of Q_{Al} and Q_{Si} remains constant when the formed silicon content is lower than 10 at.%. For example, in Fig. 10, $Q_{Si}^{Mg} > Q_{Si}^{Sc} > Q_{Si}^{Ti} > Q_{Si}^{Nb}$ at $x_{Si} = 5$ at.%, which is the same order as the beginning stage at $x_{Si} = 0$.

Therefore, after Q_{Al} and Q_{Si} are determined, ΔG_2 can be calculated as the function of content of Si released from the chemical reaction, as seen in Fig. 11. It can be seen that the Gibbs free energy of the chemical reaction changes with different alloying additions. The addition of Mg can decrease the free energy and the addition of Cu and Si can increase the free energy. Moreover, the free energy changes are greater with rising alloying element content. The corresponding silicon content of the intersecting point, where the straight line meets the dotted line ($\Delta G = 0$) in Fig. 11, represents the equilibrium silicon content that reflects the extent of the chemical reaction in Eq. (1). Therefore, it indicates that Mg addition promotes the reaction, whereas the addition of Cu or Si decreases the extent of the reaction.

The extent of the chemical reaction is proportional to the equilibrium Si content, based on Eq. (1). Therefore, the effect of alloying addition on the chemical stability can be predicted by calculating the equilibrium Si content, as seen in Fig. 12. The ordinate represents the equilibrium Si content change after alloying element addition in comparison with the SiC_p/pure Al composite at 850 °C. It indicates that most alloying additions, mainly transition metals and rare-earth elements, can reduce the chemical reaction between SiC and liquid Al. Especially the addition of La can effectively suppress the reaction. Except for Sn, most non-transition metals alloys addition, such as Sr, Zn, etc., can promote the chemical reaction and thus increase the formation of Al_4C_3.

In the extended Miedema model, the activity coefficient γ_i in infinite solution is mainly determined by f_{ij}, whose neg-

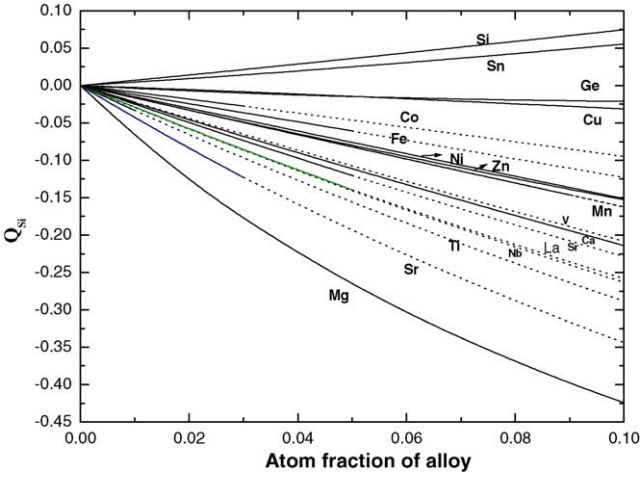

Fig. 10. Variation of Q_{Si} with adding alloy content at 850 °C (assuming Si released from the reaction is about 10 at.%).

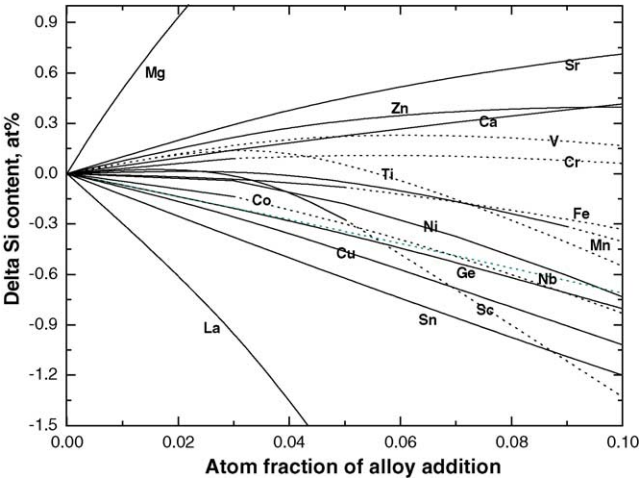

Fig. 12. Variation of equilibrium Si content with others alloys addition in Al matrix at 850 °C.

ative or positive value is dependent on the following relation: $\{q/p[(n_{ws}^{1/3})_i - (n_{ws}^{1/3})_j]^2 - (\varphi_i - \varphi_j)^2 - b(r/p)\}$. Therefore, when transition metal mixes with the non-transition liquid metals Al and Si, considering the additional large negative contribution of the value of $b(r/p)$ to f_{ij}, transition metals such as Ti, Cu, Mn, Sc, etc. have a larger effect on the activity coefficient of Al and Si than non-transition metals such as Sn, Ca, Zn, etc., due to $b(r/p) = 0$ for these non-transition alloys addition to the non-transition Al or Si melt.

In the prediction of the chemical stability, it is assumed that the added alloy cannot react with the SiC reinforcement in the molten Al matrix. But in fact, when the alloy matrix is in a liquid state, besides the interfacial reaction, the reaction between alloying element and SiC reinforcement may exist. The known alloying elements that can react with SiC and thus form carbide are Ti, V, Nb, Zr, etc. Here the reaction of Ti and SiC in molten Al matrix will be discussed in detail as a typical example.

In SiC_p/Al–Ti alloy matrix composites at high temperature, in addition to the reaction in Eq. (1) occurring, the following reaction should also be considered:

$$[Ti]_{Al} + SiC \rightarrow TiC + [Si]_{Al} \quad (20)$$

Kinetically, when SiC particles came into contact with molten aluminium, it slowly dissolved, producing silicon ions and carbon ions. These ions left the surface and migrated to the matrix by liquid-phase diffusion:

$$SiC \rightarrow [Si]_{Al} + [C]_{Al} \quad (21)$$

Then the following reactions may occur, assuming $[Ti]_{Al}$ and $[C]_{Al}$ are dilute solutes in the liquid aluminium solution:

$$[Ti]_{Al} + [C]_{Al} \rightarrow TiC \quad (22)$$

$$\frac{4}{3}[Al]_{Al} + [C]_{Al} \rightarrow \frac{1}{3}Al_4C_3 \quad (23)$$

Hence, the Gibbs free energy of the reaction (22) can be given by

$$\Delta G_3 = \Delta G_{TiC}^{f} - RT \ln a_{Ti} - RT \ln a_C \quad (24)$$

And the Gibbs free energy of the reaction (23) can be given by

$$\Delta G_4 = \frac{1}{3}\Delta G_{Al_4C_3}^{f} - \frac{4}{3}RT \ln a_{Al} - RT \ln a_C \quad (25)$$

At the beginning stage of the reaction, it is assumed that Ti is dissolved in an infinite Al solution. Therefore, referring to the data of Rapp and Zheng [28], when the weight percent of Ti is more than 0.5%, $\Delta G_3 < \Delta G_4$. It indicates that Ti is easier to react with SiC than Al and can form a more stable TiC product. Therefore, combining the calculation results of Eq. (4) with its preferred reaction with SiC particles, Ti addition (>0.5 wt.%) can reduce the chemical reaction between Al and SiC, which is in agreement with the experimental results [8].

Other alloying element that may react with SiC reinforcement and form carbide at high temperature can react similarly as Ti from a thermodynamic viewpoint. Accordingly, the effects these carbide-forming alloying elements have on the chemical stability can be attributed to the combined effects of changing the concentration, the component activity coefficient, and producing the more stable carbide.

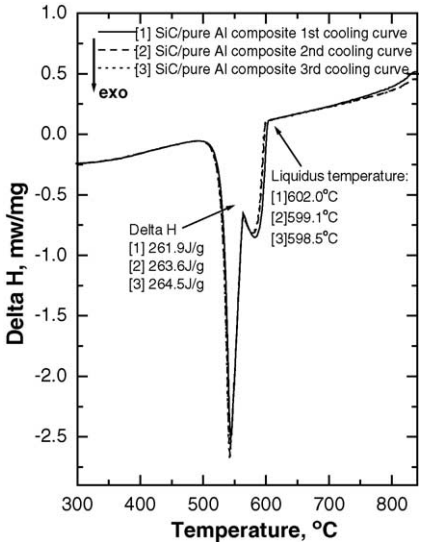

Fig. 13. Cooling curve of SiC_p/Al composites multiply remelted at 850 °C.

3.2. Experimental verification

Fig. 13 shows multiple DSC cooling curves for SiC_p/pure Al composites remelted at 850 °C. After the first remelting, all the remelt-cooling curves are nearly identical when superimposed and all the thermal parameters including the liquidus temperatures in every curve are nearly identical. Hence, it is considered that the reaction has reached equilibrium and the silicon content has reached saturation after multiple remelting [29].

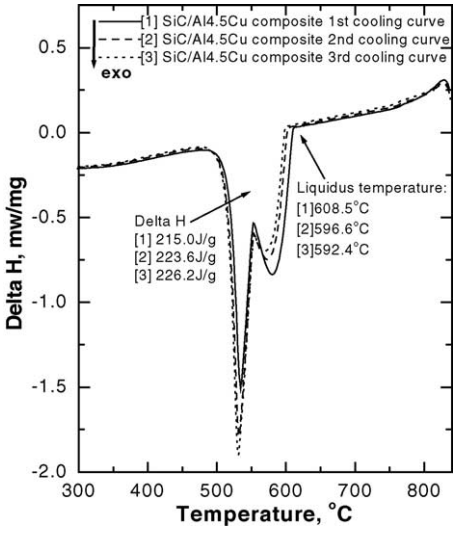

Fig. 14. Cooling curve of SiC_p/Al–4.5Cu composites multiply remelted at 850 °C.

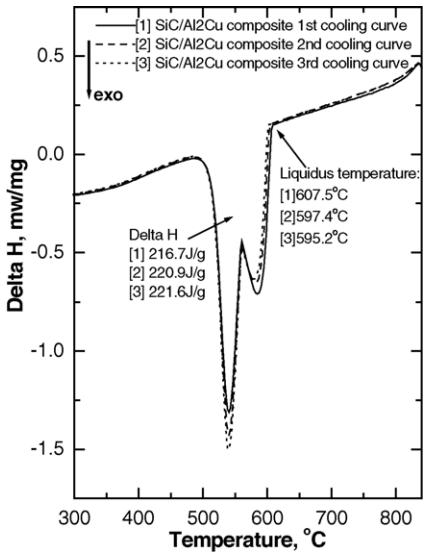

Fig. 15. Cooling curve of SiC_p/Al–2Cu composites multiply remelted at 850 °C.

Similarly, Figs. 14–17 show respectively the DSC multiple cooling curves of SiC_p/Al–4.5Cu, SiC_p/Al–2Cu, SiC_p/Al–1Mg and SiC_p/Al–4Mg composites remelted at 850 °C. As indicated in Figs. 14–17, from the thermal parameters in every cooling curve, it can be seen that after the first remelting, the interfacial reaction extent increases with increasing remelt number, although the extent increase is very small. Therefore, it is concluded that the reaction has almost reached balance after the third remelting.

The measured liquidus temperatures in the third cooling curve in Figs. 13–17 were then used to obtain Si content by the Al–Si binary phase diagram and Al–Cu–Si and Al–Mg–Si ternary vertical phase diagrams [30], as seen in Fig. 18. The

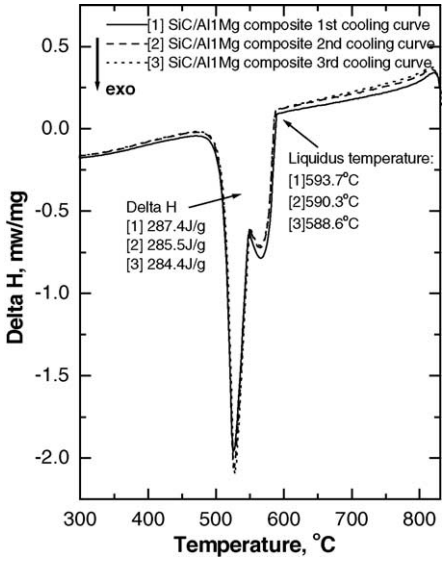

Fig. 16. Cooling curve of SiC_p/Al–1Mg composites multiply remelted at 850 °C.

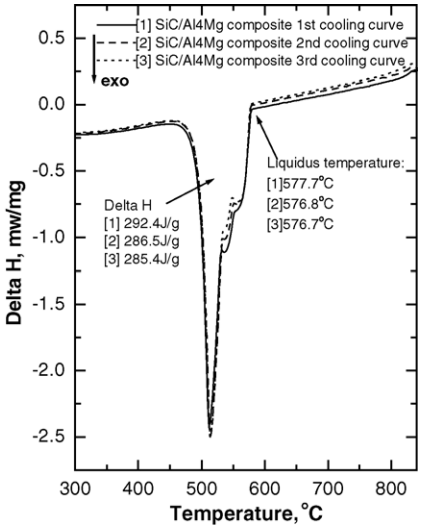

Fig. 17. Cooling curve of SiC_p/Al–4Mg composites multiply remelted at 850 °C.

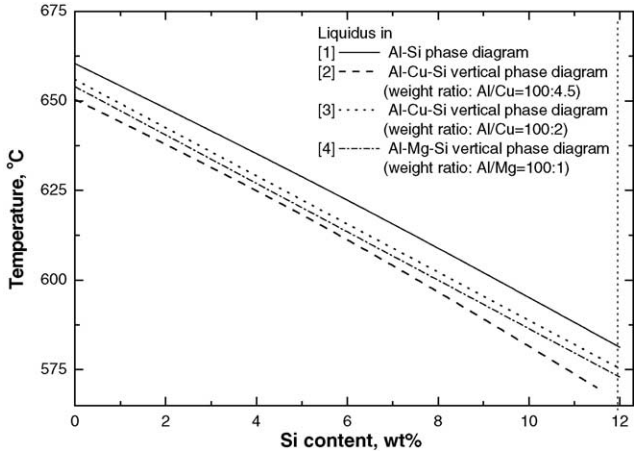

Fig. 18. Partial liquidus section of Al alloys phase diagrams.

results of the evaluated equilibrium silicon content are shown in Table 4.

Therefore, it can be deduced that in Al matrix composites reinforced by SiC particles, the addition of alloy can influence the extent of the chemical reaction between Al and SiC. Magnesium addition to the matrix can promote the reaction and the addition of copper or silicon can reduce the extent of this reaction. As seen in Fig. 19, compared with the experimental results, the calculation result shows the influence of magnesium, copper, or silicon addition on the interfacial

Table 4
The experimental results evaluated from the phase diagrams

Alloy matrix	Equilibrium Si (wt.%)
Pure Al	9.53
Al–2Cu	9.13
Al–4.5Cu	8.66
Al–1Mg	10.09
Al–4Mg	10.97

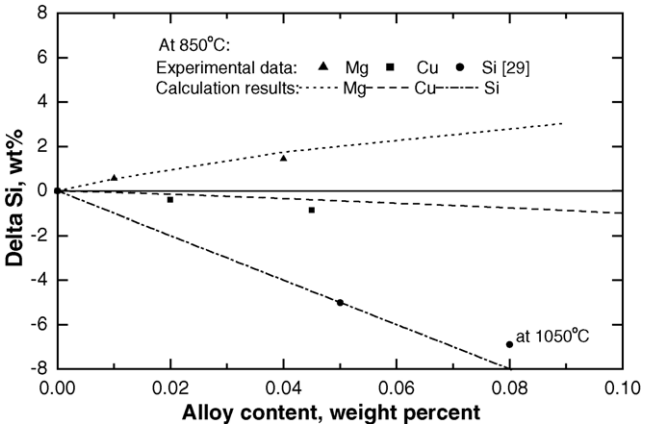

Fig. 19. Variation of equilibrium Si content from the chemical reaction with Mg or Cu addition in Al matrix.

reaction, which is in good accordance with the experimental results.

4. Conclusion

According to the calculation using an extended Miedema model and the Wilson equation, the activity coefficient changes of Al and Si were calculated with alloying element addition and thus the influence of alloying addition on the interfacial stability in SiC_p/Al at high temperature. The calculation results showed that alloying element additions such as Mg, Zn, Sr, etc. could promote the interfacial reaction and alloying addition such as Cu, Sn, Ge, La, etc. could hinder the reaction, based on the thermodynamic calculation considering the changes of the activities of reactants and products. Selecting pure Al, Al–2 wt.%Cu, Al–4.5 wt.%Cu, Al–1 wt.%Mg and Al–4 wt.%Mg, respectively, as matrices reinforced with SiC particles, the experimental results agree with the calculated results using the Wilson equation and the extended Miedema model.

Work is continuing in the applicability of this method, including the interesting possibility of theoretic prediction of the extent of in situ reactions such as Al/TiB_2, AlN/Mg and the influence of alloying addition on the formed reinforcement products in liquid multi-component alloy systems.

Acknowledgements

The authors are grateful for the finance supports of National Nature Science Foundation of People's Republic of China under the grant no. 50101006, and Major Basic Research of Shanghai under the grant no. 04DZ14002.

Appendix A

It has been proved that the Wilson equation is reliable in predicting behaviour in ternary system on the basis of the

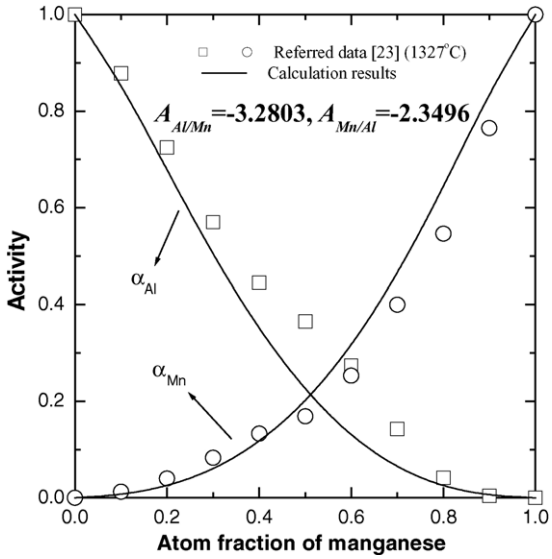

Fig. A1. Activities in liquid Al–Mn alloy at 1327 °C.

binary parameters $A_{i/j}$ and $A_{j/i}$, which were obtained to fit the binary data using the least-square method or by infinite activities coefficient [17,31–32]. Therefore, the closer the theoretically calculated activities are to that of the binary liquid alloys, the more reliable the prediction of activities in ternary liquid alloys will be, which are evaluated from the Wilson equation and extended Miedema model. Here, some thermodynamic data in binary liquid alloys are presented in Figs. A1–A6, most of which involve liquid Al alloy binary systems due to its application to SiC_p/Al alloy composites.

As seen in Figs. 1 and A1–A6, using the Wilson equation and the extended Miedema model, most of calculated activities agree well with the measured data, i.e., binary liq-

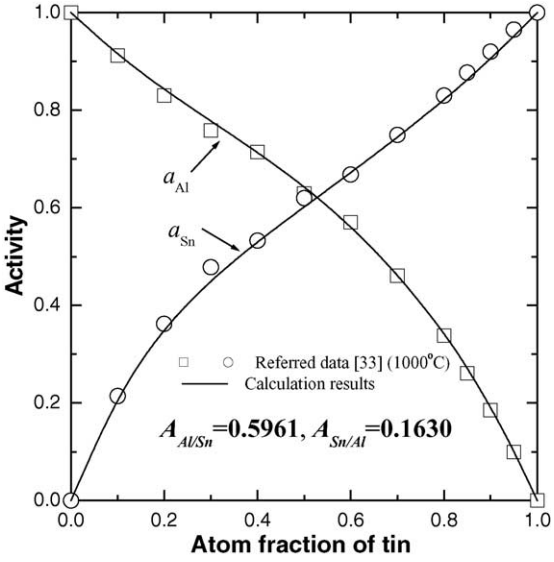

Fig. A2. Activities in liquid Al–Sn alloy at 1000 °C.

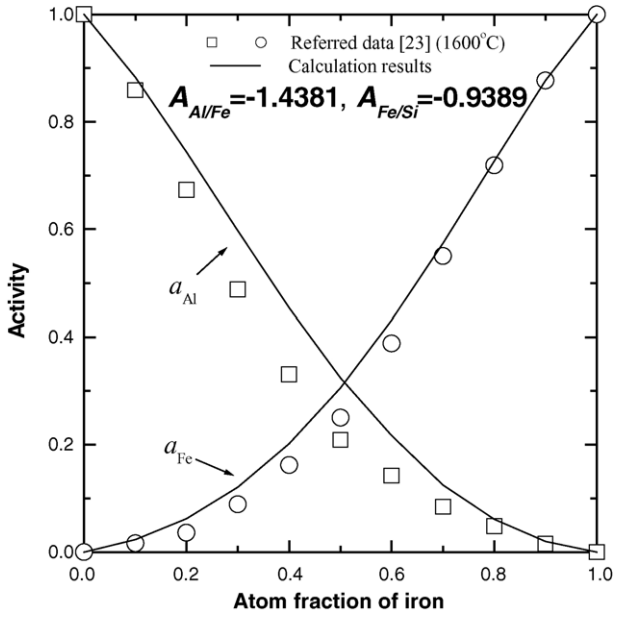

Fig. A3. Activities in liquid Al–Fe alloy at 1600 °C.

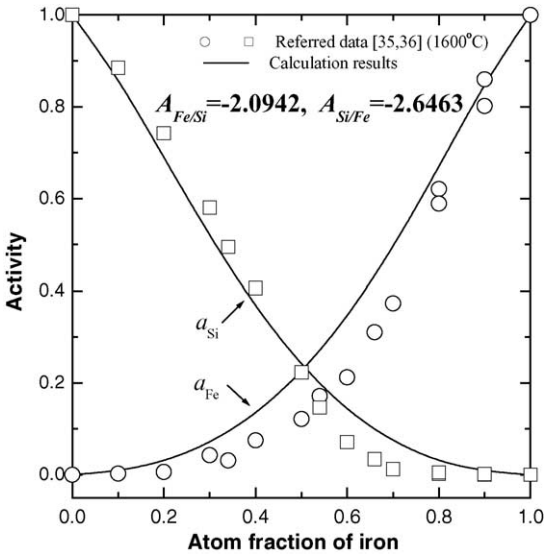

Fig. A5. Activities in liquid Fe–Si alloy at 1600 °C.

uid Al–Si, Al–Sn and Al–Mn systems [23,33]. However, a few calculated activities cannot completely the measured data in some binary alloy systems such as Al–Fe, Al–Mn and Fe–Si alloys. Nevertheless, these calculation results still are in good accordance with the trend of the activities changes with increasing alloy content. For example, as seen in Figs. A4 and A5, although there exists a few mismatches between the theoretical calculation of activity and the measured data [34–36], it can be seen that γ_{Cu} in a dilute iron solution is much more than 1 and γ_{Fe} in dilute silicon solution is much less than 1, which agrees with the influence trend evaluated from the measured data. Thus, it is believed that the prediction of the influence of alloying addition on the chemical stability is basically accurate, at least in the aspect of the trend of the influence. The deviation between calculated data and measured data primarily concentrates on the region of high concentration solute, especially when the composition of solute is in the range of 0.4–0.6. It can be ascribed that the values of parameters only depend on the activity coefficient in infinite solutions. With component concentration increasing, the complexity of interaction between atoms is

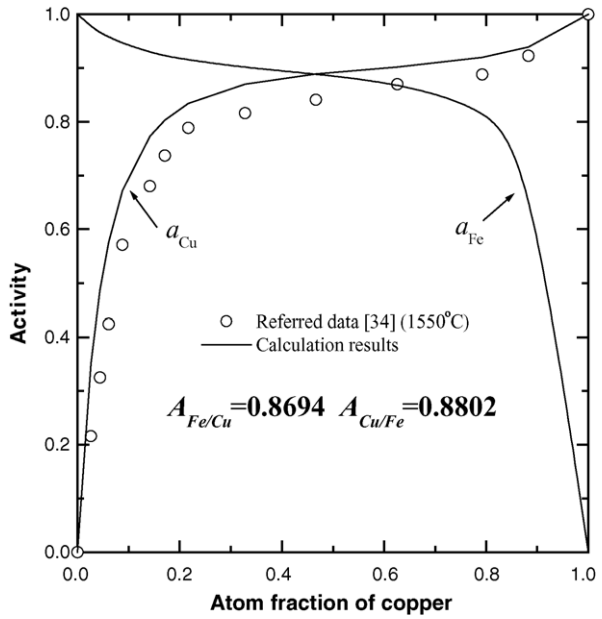

Fig. A4. Activities in liquid Fe–Cu alloy at 1550 °C.

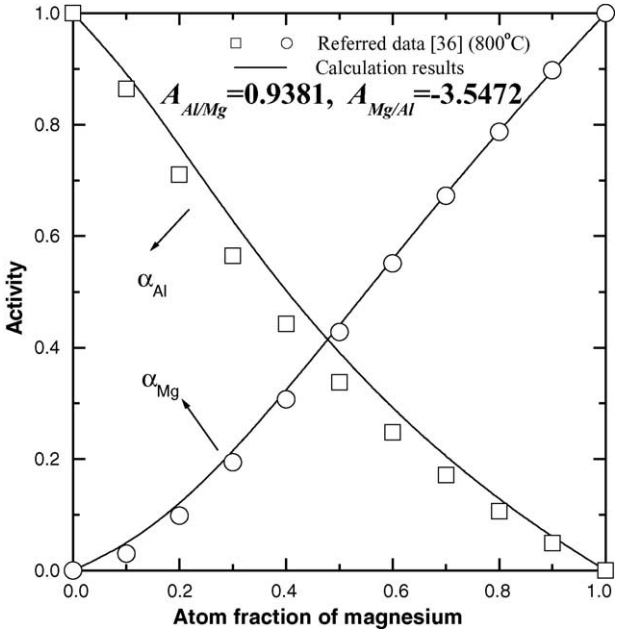

Fig. A6. Activities in liquid Al–Mg alloy at 800 °C.

ignored and the method is limited in the area of high concentration. As a result, when alloying content is not too high (<0.2), it is considered that the prediction of the chemical stability of SiC_p/Al composites at high temperature is reliable.

References

[1] A. Mortensen, I. Jin, Int. Mater. Rev. 37 (1992) 101.
[2] N. Setargew, B.A. Parker, M.J. Couper, Mater. Sci. Forum 189 (1995) 297.
[3] S. Ray, J. Mater. Sci. 28 (1993) 5397.
[4] T.X. Fan, D. Zhang, Z.L. Shi, R.J. Wu, T. Shibayanagi, M. Naka, J. Mater. Sci. 34 (1999) 5175.
[5] L.P. Lefebvre, G. L'esperance, J. Mater. Sci. 32 (1997) 3987.
[6] K. Janghorban, J. Mater. Proc. Technol. 38 (1993) 361.
[7] D.J. Lloyd, H. Lagace, Mater. Sci. Eng. A 107 (1989) 73.
[8] T.X. Fan, D. Zhang, R.J. Wu, T. Shibayanagi, M. Naka, J. Mater. Sci. Lett. 21 (2002) 1157.
[9] M. Kobashi, T. Choh, JIM 31 (1990) 1101.
[10] F. Delannay, L. Frozen, A. Deryttere, J. Mater. Sci. 22 (1987) 1.
[11] J.G. Li, L. Coudurier, N. Eustathopoulos, J. Mater. Sci. 24 (1989) 1109.
[12] N. Eustathopoulos, D. Chatain, L. Coudurier, Mater. Sci. Eng. A 135 (1991) 83.
[13] J.C. Lee, J.Y. Byun, Acta Mater. 46 (1998) 1771.
[14] J.C. Lee, S.B. Park, H.K. Seok, C.S. Oh, H.I. Lee, Acta Mater. 46 (1998) 2635.
[15] J.C. Lee, J.P. Ahn, Z.L. Shi, J.H. Shim, H.I. Lee, Metall. Trans. 32 (2001) 1541.
[16] A.R. Miedema, P.F. De Chatel, F.R. De Boer, Physica B, 100 (1980) 1.
[17] G.M. Wilson, J. Am. Chem. Soc. 86 (1964) 127.
[18] C. Simensen, Metall. Trans. A 20 (1989) 191.
[19] L. Oden, R. Mccune, Metall. Trans. A 18 (1987) 2005.
[20] J.C. Lee, J.Y. Byun, C.S. Oh, Acta Mater. 45 (1997) 5303.
[21] D.P. Tao, Metall. Mater. Trans. A 32 (2001) 1205.
[22] T. Tanaka, N.A. Gokcen, Z. Morita, Z. Metallkunde 81 (1990) 49.
[23] P.D. Desai, J. Phys. Chem. (Ref. Data) 16 (1987) 109.
[24] A.C. Ferro, B. Derby, Acta Metall. Mater. 43 (1995) 3061.
[25] J.C. Viala, P. Fortier, J. Mater. Sci. 25 (1990) 1842.
[26] I. Bari, Thermochemical Data of Pure Substances, VCH, 1989.
[27] J. Narciso, C. Garcia, E. Louis, Mater. Sci. Eng. B 15 (1992) 148.
[28] R.A. Rapp, X.J. Zheng, Metall. Trans. A 22 (1991) 3071.
[29] T.X. Fan, D. Zhang, G. Yang, Composites A 34 (2003) 291.
[30] H. Feufel, T. Gödecke, H.L. Lukas, F. Sommer, J. Alloys Compd. 247 (1997) 31.
[31] D.P. Tao, X.W. Yang, Metall. Mater. Trans. B 28 (1997) 725.
[32] D.P. Tao, X.W. Yang, Acta Metall. Sinica 33 (1997) 10.
[33] J. Blot, J. Rogez, R. Castanet, J. Less-Common Metal. 118 (1986) 67.
[34] R. Speiser, F. Jacobs, J.W. Spretnak, Trans. TMS-AIME 215 (1959) 185.
[35] L.S. Darken, Trans. TMS-AIME 239 (1967) 82.
[36] R. Hultgren, P.D. Desai, et al., Selected Values of the Thermodynamic Properties of Binary Alloys, ASM International, 1973.